Journal of Nuclear Materials 542 (2020) 152505

Contents lists available at ScienceDirect

Journal of Nuclear Materials

journal homepage: www.elsevier.com/locate/jnucmat

Tensile properties of powder-metallurgical-processed tungsten alloys after neutron irradiation near recrystallization temperatures

Takeshi Miyazawa[a,*], Lauren M. Garrison[b], Josina W. Geringer[b], John R. Echols[b], Makoto Fukuda[a,1], Yutai Katoh[b], Tatsuya Hinoki[c], Akira Hasegawa[a]

[a] Tohoku University, Sendai 980-8579, Japan
[b] Oak Ridge National Laboratory, Oak Ridge, TN 37831, USA
[c] Kyoto University, Uji 611-0011, Japan

ARTICLE INFO

Article history:
Received 2 April 2020
Revised 28 July 2020
Accepted 3 September 2020
Available online 29 September 2020

Keywords:
Polycrystalline tungsten
Tensile properties
Recrystallization
Neutron irradiation
Thermal neutron shield

ABSTRACT

The tensile properties of powder-metallurgical-processed Pure W, K-doped W, W-3%Re, and K-doped W-3%Re were examined after neutron irradiation up to 0.7 dpa at 910–1020 °C with a thermal neutron shield in the High Flux Isotope Reactor (HFIR). After irradiation, recrystallized Pure W (R) exhibited a brittle fracture mode, while recrystallized K-doped W-3%Re (R) exhibited a ductile fracture mode at 500 °C. K-doped W-3%Re (R) has fine grains, and hence, contains a considerable number of grain boundaries that act as sinks for irradiation defects. Solid solute Re in the W matrix could improve not only the mechanical properties of W, but also its resistance to neutron irradiation. At 500 °C, the ductility of K-doped W-3%Re after irradiation was significantly higher than that of Pure W. The irradiation at ~1000 °C did not induce hardening of stress-relieved (SR) W materials, but SR W materials tended to exhibit a decrease in the ultimate tensile strength (UTS) and an increase in total elongation (TE). The softening due to the recovery and recrystallization of SR W materials and the hardening due to the formation of irradiation defect clusters were balanced during irradiation at ~1000 °C, and ductility was exhibited without an increase in strength.

1. Introduction

Tungsten (W) exhibits a high melting temperature, high thermal conductivity, high resistance to sputtering, and low tritium inventory; thus, it is considered a candidate material for plasma-facing components (PFCs) for fusion reactors (for example ITER and DEMO) [1]. The divertor will be subjected to 14 MeV neutron irradiation and heat flux of 5–10 MW/m^2 during steady state operation [2–4]. In DEMO, the surface temperature of the divertor is designed to be less than the recrystallization temperature of unalloyed W (< 1300 °C) [5,6]. However, W materials will still be damaged by the heat flux, which could induce surface modification, cracking, deformation, recrystallization, and melting [7–9]. Recrystallization causes degradation of the mechanical properties of W materials in a process called recrystallization-induced embrittlement [10–12]. W materials will also be damaged by neutron irradiation, which will induce displacement damage and transmutation reactions [13]. Neutron irradiation causes neutron-irradiation-induced embrittlement, i.e., degradation of the mechanical properties of W materials [14–16]. Because both neutron irradiation and elevated temperatures can negatively affect the mechanical properties of W materials, the phase space of the temperature and neutron irradiation needs to be explored more fully to set operating limits for divertors.

Therefore, in the US-Japan collaboration project PHENIX (PFC evaluation by tritium Plasma, HEat and Neutron Irradiation eXperiments), neutron irradiation experiments using the High Flux Isotope Reactor (HFIR) were performed on various polycrystalline W and single-crystalline W materials under a wide range of irradiation temperatures. The PHENIX project has three focus areas. Task 2 in PHENIX project is focused on evaluating the neutron irradiation effects in W materials. To simulate the fusion neutron environment on neutron spectrum and irradiation temperatures, the RB-19J capsule of PHENIX had a thermal neutron shield layer made of gadolinium (Gd) inside the capsule surrounding the specimen regions, and three sub-capsules with designed target temperatures of 500 °C, 800 °C, and 1100 °C [17]. Although these irradiation temperatures are lower than the recrystallization temperature of unalloyed W, the recrystallization depends on not only temperature but

* Corresponding author.
E-mail address: takeshi.miyazawa.c7@tohoku.ac.jp (T. Miyazawa).
[1] Current Address: National Institutes for Quantum and Radiological Science and Technology, Naka 311-0193, Japan.

https://doi.org/10.1016/j.jnucmat.2020.152505
0022-3115/

also the duration time. Prof. Pantleon's group reported that rolled W materials could be recrystallized by thermal aging at around 1100 °C [18,19]. In the case of the powder-metallurgical-process-sintered W thick plates applied to the divertor tiles of fusion reactors, a new viewpoint different from that in a previous study [20] is offered by considering the mechanical properties in the neutron irradiation near recrystallization temperatures with the thermal neutron shielded capsule. Recent work by Dr. Abernethy on the fracture behavior on neutron irradiated single-crystalline W was reported [21]. The fracture work focused on ductile-to-brittle transition temperature (DBTT) for single-crystalline W by four-point bend tests. This study focused on the ductility and fracture behavior for the rolled polycrystalline W plates after neutron irradiation at high temperatures by tensile tests.

For neutron irradiation at higher temperatures, where vacancies are mobile and voids grow, an increase in volume because of void formation can also occur. Rau et al. determined the microstructure of neutron irradiated W from 1.5 to 1.6 $\times$ 10^{24} n/m^2 at 1000 °C (0.35 T_m) and 1300 °C (0.43 T_m) in the Engineering Test Reactor (ETR), and revealed void formation by neutron irradiation at higher temperatures [22]. The effects of neutron irradiation in W have been investigated using both a mixed spectrum reactor (HFIR) with a high flux of thermal neutrons and a fast spectrum fission reactor (JOYO) with a low flux of thermal neutrons. In recent studies [13,23-28], irradiation hardening in HFIR became significantly greater than that in JOYO when the fast neutron flux exceeded 1 $\times$ 10^{26} n/m^2 (E > 0.1 MeV). It is well known that these findings were due to precipitation with transmuted rhenium (Re) and osmium (Os), such as σ phase (WRe) or χ phase (WRe_3), and the irradiation-induced segregation or precipitation that occurs under neutron irradiation. Neutron irradiation in HFIR needs to use a thermal neutron shield to reduce the thermal neutron flux to be similar to the level expected in a fusion reactor. Moreover, neutron irradiation experiments conducted at a maximum temperature of 800 °C were the main focus in previous studies [13,23–28], and there were few experimental data at a 1000 °C irradiation temperature, which is near the recrystallization temperature of unalloyed W [13,22,27]. Therefore, neutron irradiation experiments in this study were carried out at high temperatures within 910–1020 °C to investigate neutron irradiation effects near the recrystallization temperatures.

Prof. Hasegawa's group developed neutron-irradiation-tolerant W materials modified by potassium (K) doping and Re addition [29,30]. The powder metallurgy method was adopted to fabricate the W materials of divertor tiles for mass production with microstructural uniformity. One of the features of the W rolled plates produced by powder metallurgy is that their grain size and structure can be controlled by the deformation ratio and alloying. A layered structure in which grains have a pancake shape was formed by rolling. The elastic strain, which is introduced by the worked dislocations of the rolling process, should be moderated by a stress-relieved (SR) treatment where the worked dislocations are partially recovered to form cell structures in the grain [31,32]. These microstructure controls are effective in suppressing the low-temperature embrittlement of W materials. Prof. Nogami et al. found that K-doping and 3%Re addition could produce a lower DBTT and higher upper shelf energy than those of Pure W [29]. In addition, K-doping and 3%Re addition can increase the recrystallization temperature and high-temperature strength to 1000 °C or higher [30,33]. Moreover, it is expected that neutron-irradiation-induced embrittlement can be suppressed by grain refining due to K-doping because grain refining increases the number of grain boundaries that act as sinks for irradiation defects.

The purpose of this study is to investigate the effectiveness of K-doping and Re addition in W materials in a neutron irradiation environment simulating a fusion reactor, and understand their usability in a wide range of operating temperatures in fusion reactors from an engineering viewpoint.

Table 1
Chemical compositions of Pure W, K-doped W, W-3%Re and K-doped W-3%Re plates [29,34–37].

Chemical composition	Pure W	K-doped W	W-3%Re	K-doped W-3%Re
Re (mass%)	–	–	3.0	3.0
K (ppm)	< 5	30	< 5	28
Al (ppm)	< 2	15	2	19
Si (ppm)	< 5	17	< 5	20
C (ppm)	10	10	< 10	10
N (ppm)	< 10	< 10	< 10	< 10
O (ppm)	< 10	< 10	< 10	< 10

2. Experimental procedures

2.1. Materials and grain structure

Pure W, K-doped W, W-3%Re, and K-doped W-3%Re plates (the percentages represent the nominal mass ratio of Re in the alloys) with a thickness of 7 mm were examined in this work. They were fabricated via powder metallurgy (cold isostatic pressing at room temperature and sintering at 1800–2200 °C) and hot rolling at 1400–1600 °C followed by heat treatment at 900 °C for 20 min for stress relief. The reduction ratio (deformation ratio) for the hot rolling of the four plates was the same. All four plates were supplied by A.L.M.T. corp, Japan in as-received condition, which includes the stress relief treatment. To clarify what type of heat treatment the materials had, each material label contains either "SR" to signify the as-received stress relieved condition, "R" to signify recrystallized material, or "TA" to signify the thermal aged material. The chemical composition in SR plates are listed in Table 1. Detailed descriptions of the materials, such as the fabrication process, are provided in the literature [29,34–37]. Recrystallized Pure W (R) and K-doped W-3%Re (R) were prepared from Pure W (SR) and K-doped W-3%Re (SR), respectively, by annealing at 1500 °C for 1 h. To understand the thermal aging effect during irradiation, long-term annealed Pure W (TA), K-doped W (TA), W-3%Re (TA), and K-doped W-3%Re (TA) were also prepared from Pure W (SR), K-doped W (SR), W-3%Re (SR), and K-doped W-3%Re (SR), respectively, by thermal aging at 1100 °C for approximately 3000 h [33]. TA W materials were prepared to simulate the thermal history for the high temperature irradiation period. The average grain sizes along L, T, and S directions (d_L, d_T, and d_S) of Pure W and its alloys in stress-relieved or recrystallized conditions are summarized in Fig. 1. The L, T, and S directions correspond to the rolling direction of the plate, normal to the rolling direction, and perpendicular to both L and T, respectively. The grain sizes were measured according to the ASTM E112-85 standard [38]. The SR W plates had layered grain structures in which grains were flattened along the rolling direction. Recrystallized W plates had equiaxial grain structures owing to the recrystallization.

2.2. Neutron irradiation

To simulate the fusion neutron environment on neutron spectrum, an irradiation capsule (RB-19J capsule hereafter) with thermal neutron shield was designed and irradiated in HFIR at Oak Ridge National Laboratory (ORNL). The RB-19J capsule located in the removable beryllium (RB) outer ring of the HFIR [39,40]. The neutron energy spectra for the beginning of the first cycle in RB-19J capsule were calculated by the thermal neutron shield design [39]. The Gd shield was highly effective to reduce the thermal neutron flux. The neutron irradiation conditions in this study are listed

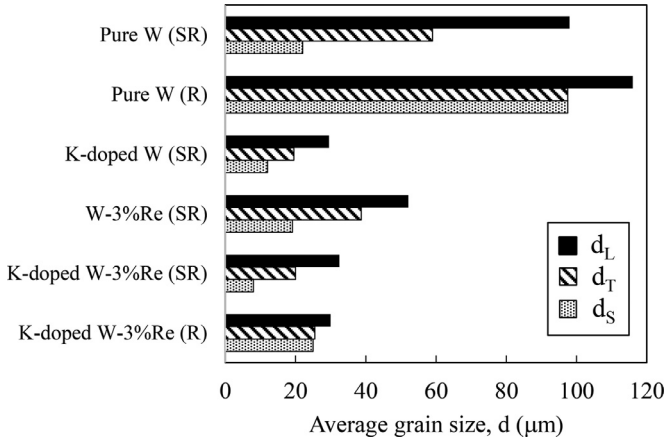

Fig. 1. Average grain sizes along the L, T, and S directions (d_L, d_T, and d_S) of Pure W and its alloys in stress-relieved or recrystallized conditions [29,36,37].

in Table 2. The actual irradiation temperatures were within 910-1020°C, and the mean fast neutron fluences were 3.4–3.7 × 10^{25} n/m^2 (E_n > 0.1 MeV). A fast neutron fluence of 1 × 10^{25} n/m^2 corresponds to approximately 0.2 dpa in W [41]. Solid transmutation rates of Re and Os in Pure W during HFIR irradiations in unshielded (Flux Trap) and shielded (RB-19J) capsules were estimated to be 8.4 %/dpa and 3.2 %/dpa, and ~0.7 %/dpa and ~0 %/dpa, respectively [13,42]. Detailed experimental procedures for neutron irradiation, such as temperature monitors and irradiation period, have been reported previously [20].

2.3. Tensile test

To investigate the tensile properties of yield stress (YS), ultimate tensile strength (UTS), uniform elongation (UE), total elongation (TE), and reduction in area (RA) of the irradiated Pure W and its alloys, tensile tests were conducted at the Low Activation Materials Development and Analysis (LAMDA) laboratory in ORNL. Flat-plate specimens, which are also called SS-J2 tensile specimens, were used for the tensile tests. They had a gauge length of 5 mm, gauge width of 1.2 mm, and thickness of 0.5 mm. Specimens were cut out from the plates using electrical discharge machining (EDM), and their surface was mechanically polished along their loading axis with emery paper with a roughness number of #1500. The loading axis of the specimens was parallel to the L direction (rolling direction) of the plates. Tensile tests along the L direction were conducted in a vacuum with a pressure less than 6.0 × 10^{-3} Pa at an initial strain rate of 1.7 × 10^{-3}/s by using an MTS Insight 30 test frame. The test temperatures were 500 °C and 900 °C. A fixture made of Inconel was used for tests at 500 °C to estimate the low-temperature ductility of the irradiated W materials. A fixture made of alumina for the MTS Insight 30 test frame at LAMDA was fabricated to conduct high-temperature tests at 900 °C, which was slightly lower than the irradiation temperatures of 910-1020 °C. A tensile test for an unirradiated specimen of Pure W (R) was conducted in a vacuum below 3.0 × 10^{-3} Pa at 900 °C at an initial strain rate of 3.3 × 10^{-2}/s by using a CATY-T3HSt/HV13 (Yonekura MFG Co., Ltd., Japan) electromotive testing machine at Tohoku University. The tensile tests were performed without an extensometer; therefore, crosshead displacement was used to calculate the strain. This method adds machine compliance error in the elastic region of the data, but it has minimal effect on the strength and strain values after yielding. One sample was tested for each test condition. The ruptured surfaces were observed using scanning electron microscopy (SEM) to evaluate the RA and to clarify the fracture mode.

3. Results

3.1. Tensile properties tested at 900 °C

Fig. 2 summarizes the engineering stress–strain curves of various Pure W materials before and after irradiation tested at 900 °C. Unirradiated Pure W (SR) exhibited good elongation and high strength because the TE and UTS were 15.0 % and 472 MPa, respectively. However, unirradiated Pure W (TA) evidenced great elongation but low strength because unirradiated Pure W (TA) was a primary recrystallized material owing to thermal aging [33]. Unirra-

Table 2
Irradiation conditions and a summary of the tensile properties of unirradiated and irradiated W materials.

Sample ID	Material type	Irradiation temperature [°C]	Fluence [10^{25} n/m^2 (E>0.1 MeV))]	dose [dpa]	Test temperature [°C]	YS [MPa]	UTS [MPa]	UE [%]	TE [%]	RA [%]
Unirrad.	Pure W (SR)	–	–	–	900	441	472	1.2	15.0	84
Unirrad.	Pure W (TA)	–	–	–	900	91	212	46.2	67.4	90
P00G	Pure W (SR)	1000	3.67	0.72	900	311	456	8.0	25.7	85
Unirrad.	Pure W (SR)	–	–	–	500	525	533	1.7	13.3	70
Unirrad.	Pure W (TA)	–	–	–	500	141	285	45.4	63.5	82
P00H	Pure W (SR)	1000	3.66	0.71	500	354	474	9.1	23.1	83
X00G	Pure W (R)	920	3.44	0.67	900	341	446	4.3	10.3	59
X00H	Pure W (R)	910	3.43	0.67	500	0	374	0	0	0
Unirrad.	K-doped W (SR)	–	–	–	900	534	544	0.5	11.3	–
Unirrad.	K-doped W (TA)	–	–	–	900	130	262	43.1	67.9	–
600G	K-doped W (SR)	980	3.54	0.69	900	412	495	10.6	25.6	73
Unirrad.	W-3%Re (SR)	–	–	–	900	476	527	1.9	10.9	–
Unirrad.	W-3%Re (TA)	–	–	–	900	450	492	5.0	15.5	78
410G	W-3%Re (SR)	1010	3.59	0.70	900	436	559	4.7	14.3	65
Unirrad.	W-3%Re (SR)	–	–	–	500	593	656	7.2	18.2	–
Unirrad.	W-3%Re (TA)	–	–	–	500	534	609	11.1	18.4	62
410H	W-3%Re (SR)	1010	3.58	0.70	500	462	590	7.4	7.6	0
Unirrad.	K-doped W-3%Re (SR)	–	–	–	900	623	641	0.5	8.6	–
Unirrad.	K-doped W-3%Re (TA)	–	–	–	900	529	560	6.6	20.0	73
800G	K-doped W-3%Re (SR)	1010	3.63	0.71	900	464	569	8.4	19.0	76
Unirrad.	K-doped W-3%Re (SR)	–	–	–	500	709	775	5.4	14.4	–
Unirrad.	K-doped W-3%Re (TA)	–	–	–	500	622	695	11.8	22.0	58
800H	K-doped W-3%Re (SR)	1020	3.36	0.71	500	484	588	14.7	25.0	67
700G	K-doped W-3%Re (R)	950	3.50	0.68	900	526	605	6.0	16.3	69
700H	K-doped W-3%Re (R)	940	3.49	0.68	500	566	671	9.4	18.2	70

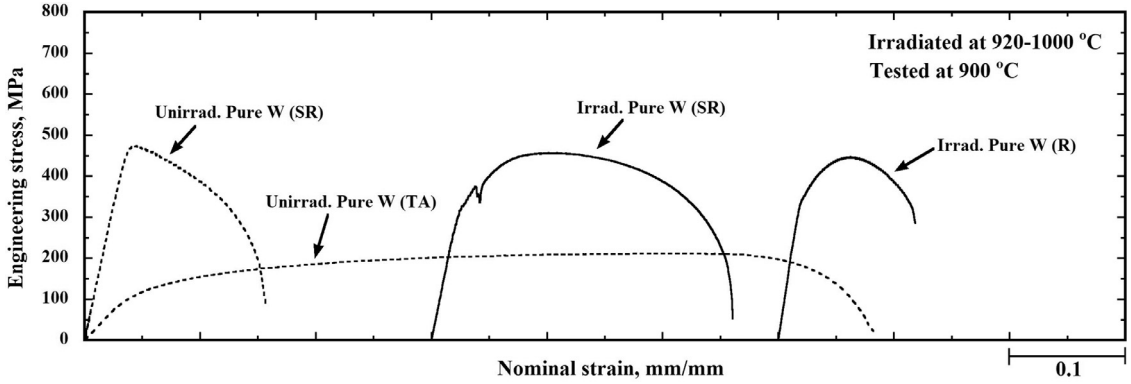

Fig. 2. Stress–strain curves of Pure W before and after irradiation tested at 900 °C. The test temperature of 900 °C was about 100 °C lower than the irradiation temperatures of 920–1000 °C.

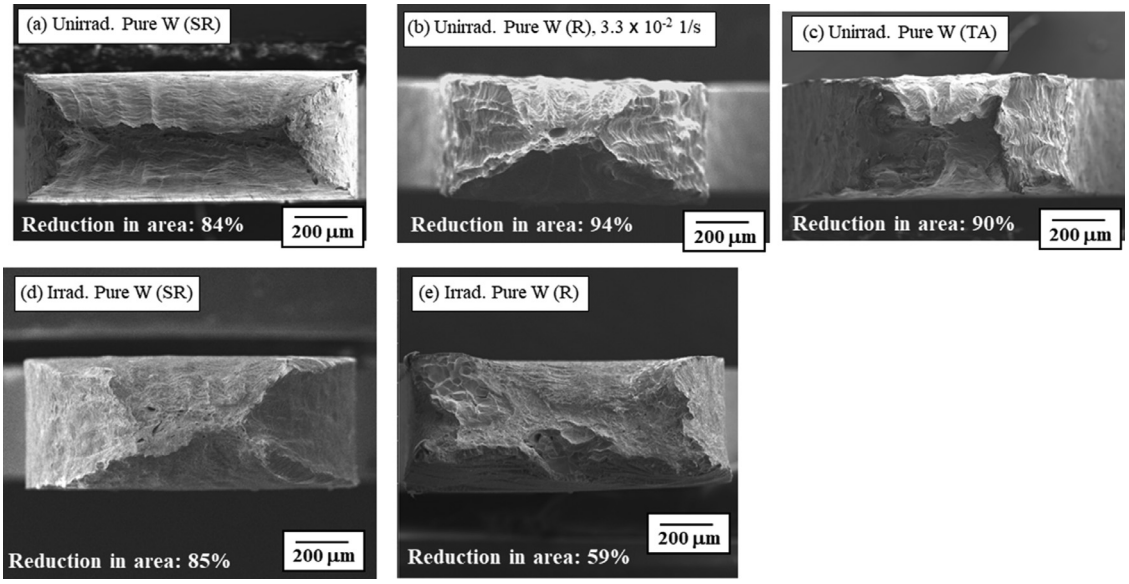

Fig. 3. SEM images of the ruptured surfaces after tensile tests at 900 °C of (a) unirradiated Pure W (SR), (b) unirradiated Pure W (R), (c) unirradiated Pure W (TA), (d) irradiated Pure W (SR), and (e) irradiated Pure W (R). Irradiation temperatures were 920–1000 °C.

diated K-doped W (TA) also exhibited the same tensile properties as unirradiated Pure W as shown in Table 2. This is because K-doped W (TA) is also a recrystallized material following thermal aging [33]. Comparing Pure W (SR) before and after irradiation, irradiated Pure W (SR) had a higher elongation and lower YS than unirradiated Pure W (SR). Comparing irradiated Pure W in the SR and R conditions, irradiated Pure W (R) showed the same strength as irradiated Pure W (SR), but the elongation of irradiated Pure W (R) was reduced by less than half compared to that of irradiated Pure W (SR). The stress–strain curve of irradiated Pure W (SR) showed a rapid decrease in stress (a jog in the curve) at a strain of 0.04 mm/mm. This is likely due to the sliding that occurs at the contact surface between the fixture and shoulder of the SS-J2 specimen. Figs. 3 and 4 show the ruptured surface of Pure W materials before and after irradiation, tested at 900 °C. First, a necking deformation of unirradiated Pure W materials can be noticed. Pure W (SR) is characterized by large deformation in the thickness direction during necking, because it has a layered structure formed by hot rolling. However, Pure W (R) and Pure W (TA) are characterized by deformations in the thickness and width directions during necking, because they have an equiaxial grain structure owing to primary recrystallization. Comparing the necking deformation of Pure W (SR) before and after irradiation, while unirradiated Pure W (SR) had primarily deformation in the thickness direction, irradiated Pure W (SR) was characterized by deformations in the thickness and width directions during necking. Dimples were observed in the fractographs, not only in unirradiated Pure W (SR) but also irradiated Pure W (SR) that had an RA of over 80 %, which is typical for a ductile fracture. Dimples and an intergranular fracture were observed on the fractograph of irradiated Pure W (R).

Fig. 5 summarizes the engineering stress–strain curves of various K-doped W-3%Re materials before and after irradiation tested at 900 °C. Unirradiated K-doped W-3%Re (SR) exhibited good elongation and superior strength because the TE and UTS were 8.6 % and 641 MPa, respectively. The strength of K-doped W-3%Re (TA) was lower than that of K-doped W-3%Re (SR), but the elongation of K-doped W-3%Re (TA) was higher than that of K-doped W-3%Re (SR) because unirradiated K-doped W-3%Re (TA) was in a recovered state owing to thermal aging [33]. Unirradiated W-3%Re (TA) also exhibited the same tensile properties as unirradiated K-doped

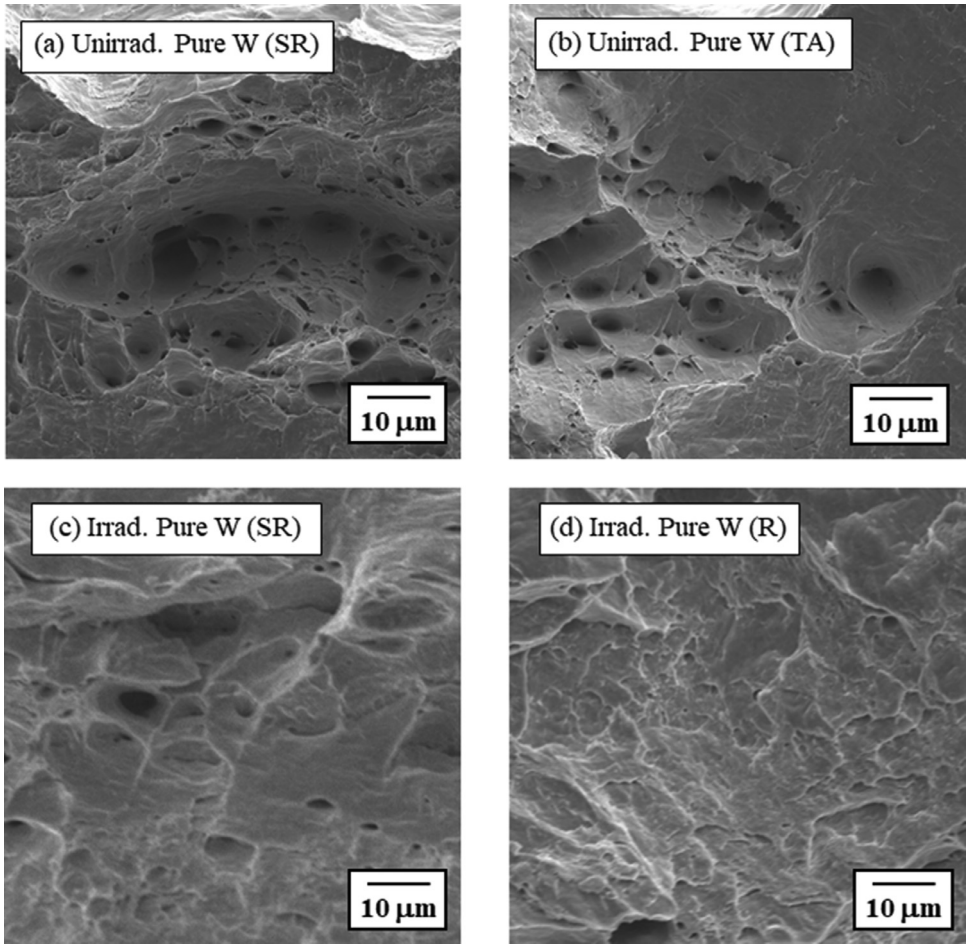

Fig. 4. High magnification SEM images of the ruptured surfaces after tensile tests at 900 °C of (a) unirradiated Pure W (SR), (b) unirradiated Pure W (TA), (c) irradiated Pure W (SR), and (d) irradiated Pure W (R). Irradiation temperatures were 920–1000 °C.

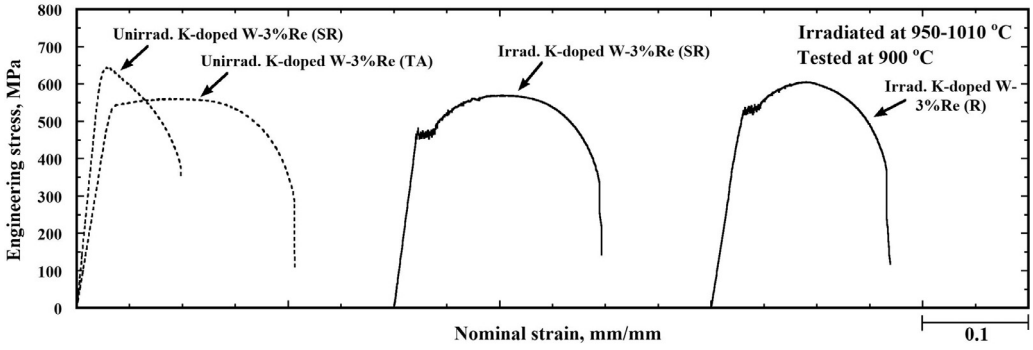

Fig. 5. Stress–strain curves of K-doped W-3%Re before and after irradiation tested at 900 °C. The test temperature of 900 °C was about 100 °C lower than the irradiation temperatures of 950-1010 °C.

W-3%Re (TA) as shown in Table 2, because of the recovery of the thermal aging of W-3%Re (TA) [33]. The addition of 3%Re was effective in improving the recrystallization temperature of W materials. Figs. 6 and 7 show the ruptured surface of K-doped W-3%Re materials before and after irradiation. K-doped W-3%Re (TA) is characterized by large deformations in the thickness direction during necking, because it maintains a layered structure after thermal aging. Irradiated K-doped W-3%Re materials are also characterized by large deformations in the thickness direction during necking. Dimples were observed on the fractographs of irradiated K-doped W-3%Re materials, which is typical for ductile fracture.

3.2. Tensile properties tested at 500 °C

Fig. 8 summarizes the engineering stress–strain curves of various Pure W materials before and after irradiation tested at 500 °C.

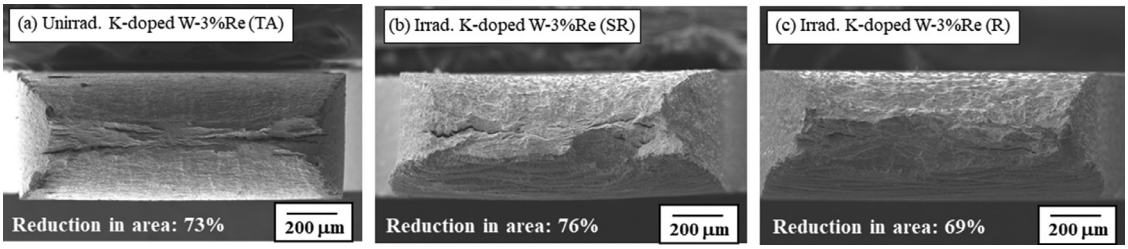

Fig. 6. SEM images of the ruptured surfaces after tensile tests at 900 °C of (a) unirradiated K-doped W-3%Re (TA), (b) irradiated K-doped W-3%Re (SR), and (c) irradiated K-doped W-3%Re (R). Irradiation temperatures were 950–1010 °C.

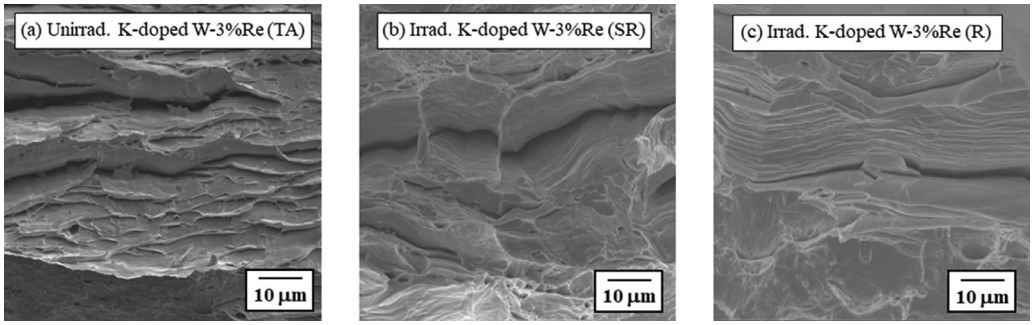

Fig. 7. High magnification SEM images of the ruptured surfaces after tensile tests at 900 °C of (a) unirradiated K-doped W-3%Re (TA), (b) irradiated K-doped W-3%Re (SR), and (c) irradiated K-doped W-3%Re (R). Irradiation temperatures were 950–1010 °C.

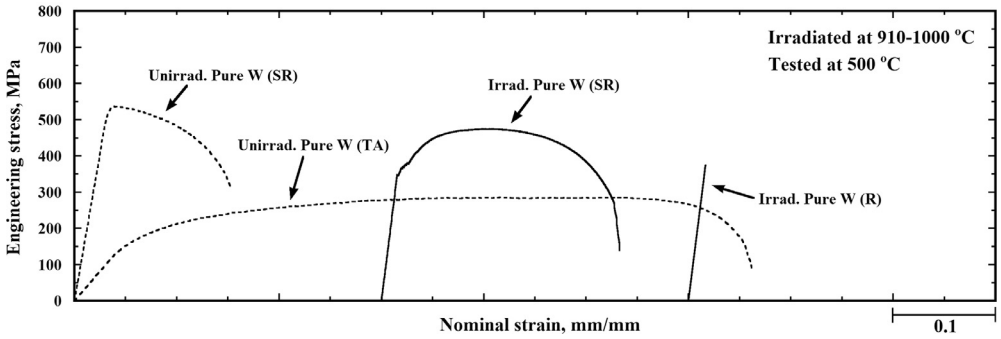

Fig. 8. Stress–strain curves of Pure W before and after irradiation tested at 500 °C. The test temperature of 500 °C was much lower than the irradiation temperatures of 910-1000 °C.

Unirradiated Pure W (SR) exhibited good elongation and high strength because the TE and UTS were 13.3 % and 533 MPa, respectively. However, unirradiated Pure W (TA) demonstrated great elongation but low strength because unirradiated Pure W (TA) is a primary recrystallized material by thermal aging [33]. Comparing Pure W (SR) before and after irradiation, irradiated Pure W (SR) had higher elongation and lower YS than those of unirradiated Pure W (SR). However, irradiated Pure W (R) ruptured in the elastic region without yielding. Figs. 9 and 10 show the ruptured surface of Pure W materials before and after irradiation tested at 500 °C. Pure W (SR) is characterized by large deformation in the thickness direction during necking because it has a layered structure due to hot rolling. However, Pure W (TA) is characterized by deformations in the thickness and width directions during necking because it has an equiaxial grain structure due to primary recrystallization. Comparing the necking deformation of Pure W (SR) before and after irradiation, irradiated Pure W (SR) is characterized by deformation in the thickness and width directions during necking. Dimples were observed in the fractographs of irradiated Pure W (SR) that had an RA of over 80 %, which is typical for ductile fracture. However, irradiated Pure W (R) exhibited intergranular fracture and no necking. It exhibited a typical brittle fracture mode. It is possible that the irradiation-induced hardening is caused by the formation of irradiation defects (voids and dislocation loops) in the matrix. As the grain interiors hardens, the strength of the grain boundaries relatively decreases; subsequently, an intergranular fracture occurs.

Fig. 11 summarizes the engineering stress–strain curves of various K-doped W-3%Re materials before and after irradiation tested at 500 °C. Unirradiated K-doped W-3%Re (SR) demonstrated good elongation and superior strength because the TE and UTS were 14.4 % and 775 MPa, respectively. The strength of K-doped W-3%Re (TA) was lower than that of K-doped W-3%Re (SR), but the elongation of K-doped W-3%Re (TA) was higher than that of K-doped W-3%Re (SR) because unirradiated K-doped W-3%Re (TA) is in a recovered

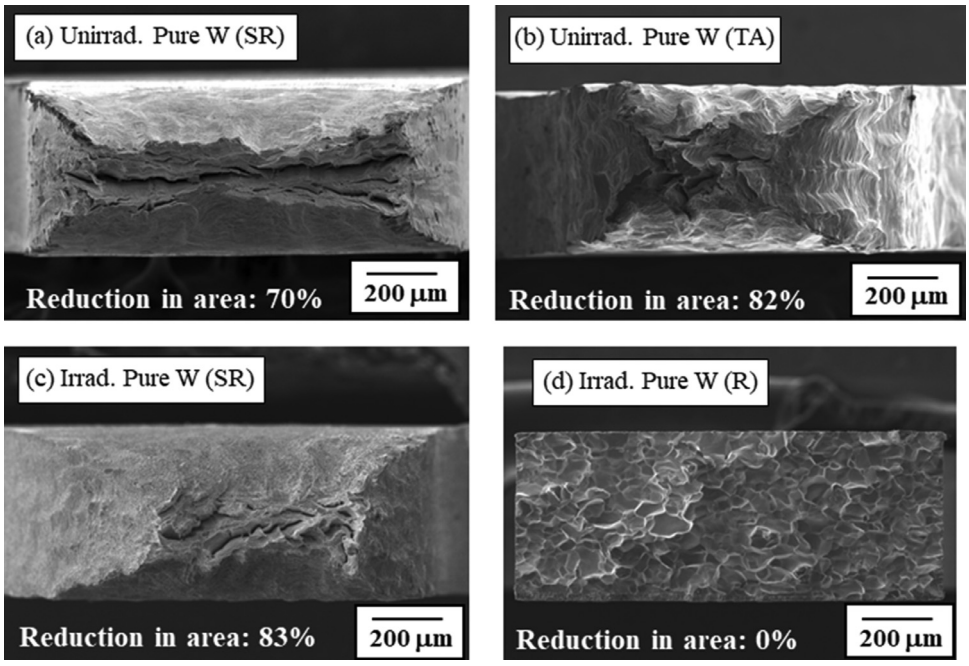

Fig. 9. SEM images of the ruptured surfaces after tensile tests at 500 °C for (a) unirradiated Pure W (SR), (b) unirradiated Pure W (TA), (c) irradiated Pure W (SR) and (d) irradiated Pure W (R). Irradiation temperatures were 910–1000 °C. A fractograph of unirradiated Pure W (SR) has been published [20].

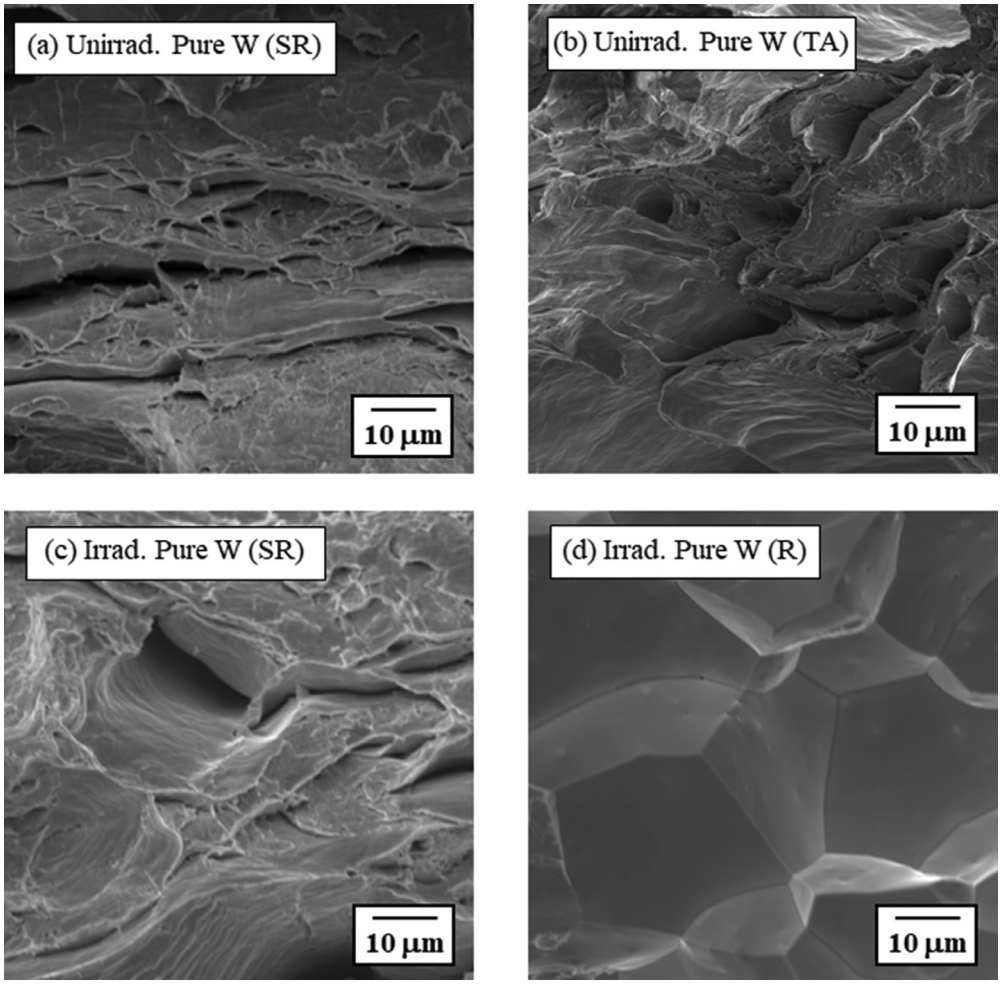

Fig. 10. High magnification SEM images of the ruptured surfaces after tensile tests at 500 °C for (a) unirradiated Pure W (SR), (b) unirradiated Pure W (TA), (c) irradiated Pure W (SR) and (d) irradiated Pure W (R). Irradiation temperatures were 910–1000 °C. A fractograph of unirradiated Pure W (SR) has been published [20].

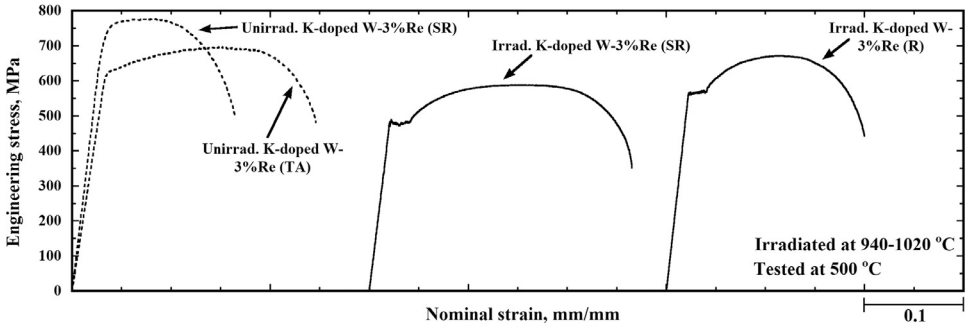

Fig. 11. Stress–strain curves of K-doped W-3%Re before and after irradiation tested at 500 °C. The test temperature of 500 °C was much lower than the irradiation temperatures of 940–1020 °C.

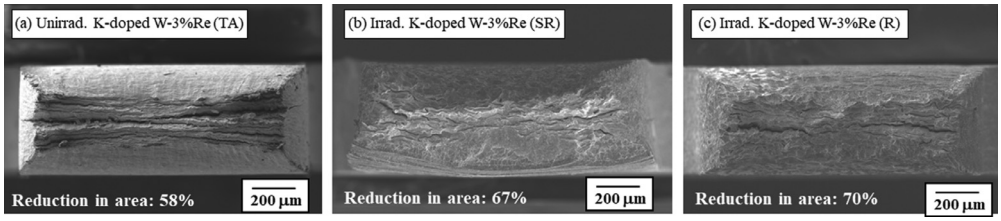

Fig. 12. SEM images of the ruptured surfaces after tensile tests at 500 °C of (a) unirradiated K-doped W-3%Re (TA), (b) irradiated K-doped W-3%Re (SR) and (c) irradiated K-doped W-3%Re (R). Irradiation temperatures were 940–1020 °C.

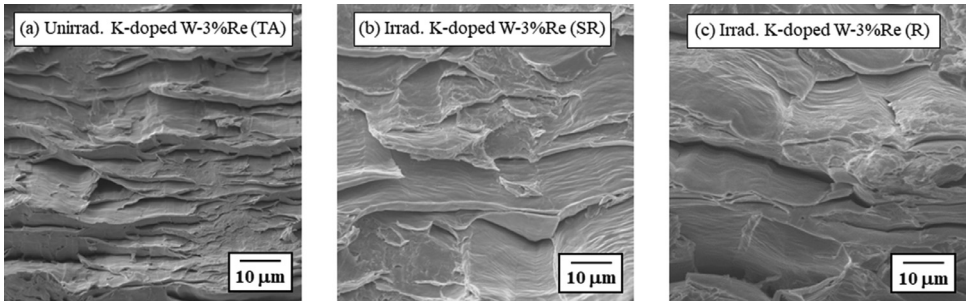

Fig. 13. High magnification SEM images of the ruptured surfaces after tensile tests at 500 °C of (a) unirradiated K-doped W-3%Re (TA), (b) irradiated K-doped W-3%Re (SR) and (c) irradiated K-doped W-3%Re (R). Irradiation temperatures were 940–1020 °C.

state owing to thermal aging [33]. Unirradiated W-3%Re (TA) also exhibited the same tensile properties as unirradiated K-doped W-3%Re (TA) as shown in Table 2, because W-3%Re (TA) is also in a recovered state owing to thermal aging [33]. Figs. 12 and 13 show the ruptured surface of K-doped W-3%Re materials before and after irradiation tested at 500 °C. K-doped W-3%Re (TA) is characterized by large deformation in the thickness direction during necking because it maintains a layered structure after thermal aging. Irradiated K-doped W-3%Re materials are also characterized by large deformation in the thickness direction during necking. Dimples were observed in the fractographs of irradiated K-doped W-3%Re materials, which is typical for ductile fracture even at a relatively low-temperature of 500 °C.

3.3. Dependence of tensile properties on irradiation temperatures for stress-relieved W materials

Figs. 14 and 15 summarize the dependence of tensile properties on irradiation temperatures for W materials (SR). When the irradiation temperatures ranged from ~600 °C to ~800 °C (test temperatures 500 °C and 700 °C respectively), the tensile strength approximately doubled and elongation decreased, which indicates that irradiation hardening occurred. However, samples irradiated at ~800 °C also received approximately double the neutron dose as those irradiated at ~500 °C. At the irradiation temperature of ~1000 °C in this study, hardening was not induced; rather, a decrease in tensile strength was observed. The samples irradiated at 910–1020 °C received approximately the same dose as those irradiated at ~800 °C. The softening was due to the recovery and recrystallization during high-temperature irradiation. More detailed research is needed to clarify the mechanism through which softening of the microstructure and grain structure of W materials (SR) occurs for irradiation at 910–1020 °C.

4. Discussion

A comparison of the tensile properties of recrystallized Pure W and K-doped W-3%Re tested at 500 °C revealed that Pure W (R)

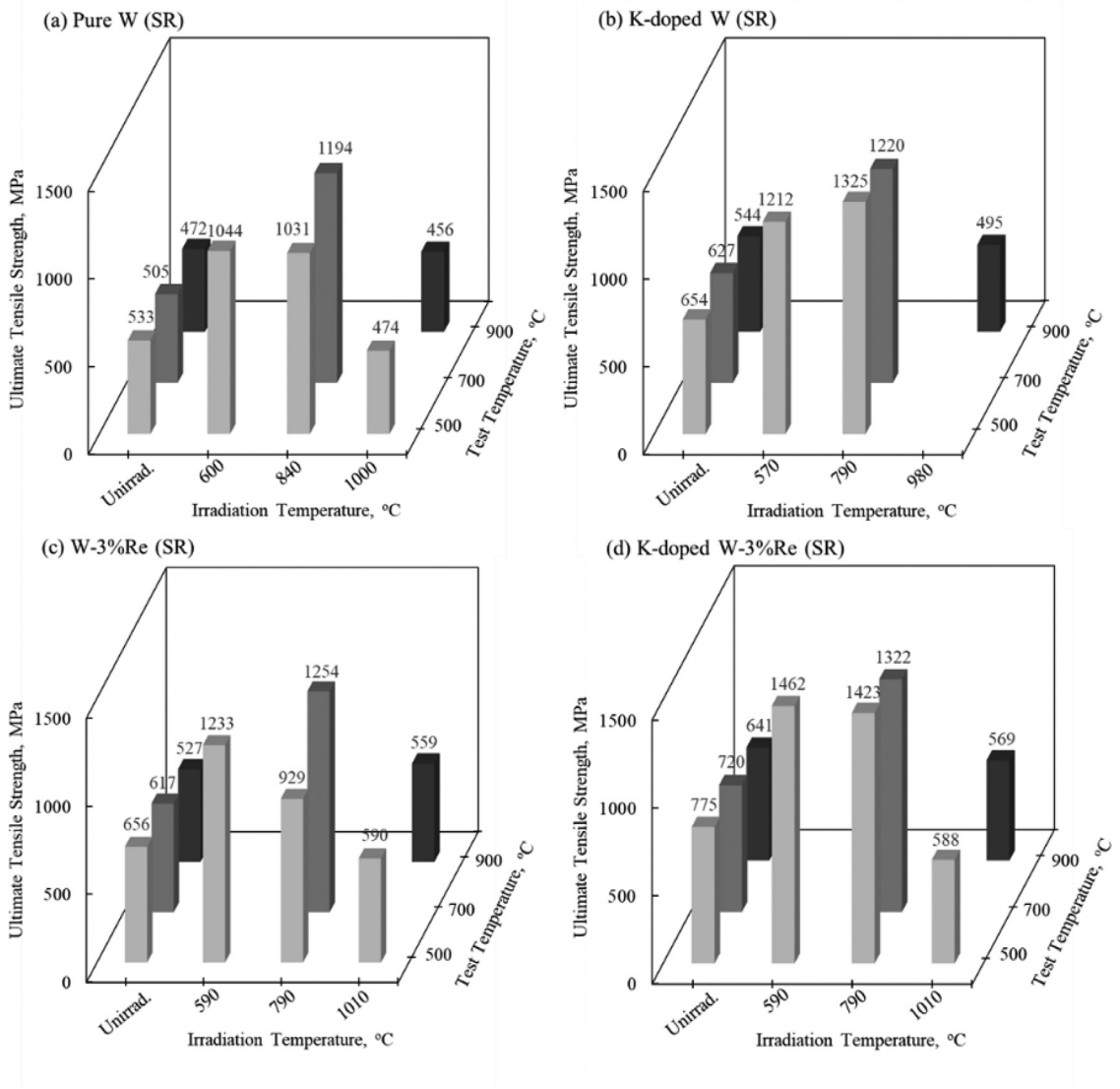

Fig. 14. Dependence of ultimate tensile strength on irradiation temperatures. Test temperatures were about 100 °C lower than the irradiation temperatures. Tensile data of Pure W and its alloys irradiated at ~600 °C and ~800 °C have been published [20].

exhibited a brittle fracture, while K-doped W-3%Re (R) exhibited a ductile fracture. It is possible that the irradiation-induced hardening is caused by the formation of irradiation defects (voids and dislocation loops) in the matrix of both Pure W (R) and K-doped W-3%Re (R). As the grain interior hardens, the strength of the grain boundaries decreases, and subsequently, an intergranular fracture occurs in Pure W (R). K-doped W-3%Re (R) experiences two positive effects due to K-doping and 3%Re addition that improve irradiation resistance. K-doping can produce finer grains compared to Pure W, as shown in Fig. 1, because K bubbles inhibit grain boundary migration in general [43]. Furthermore, as K-doped W-3%Re (R) contains fine grains, it also contains a considerable amount of grain boundaries that act as sinks for defects formed by neutron irradiation. Solid solute Re in the W matrix could improve not only the mechanical properties of W but also its resistance to recrystallization and neutron irradiation. Re in W could cause solid solution strengthening at high temperature and solid solution softening at low temperature [44]. An addition of 3%Re could be effective in increasing the work hardening coefficient, which would result in an increase in UE [37]. Therefore, a 3%Re addition could improve ductility at 500 °C. It was reported that solid solute Re is effective in suppressing void and dislocation loop formation [45]. Consequently, the ductility of K-doped W-3%Re at 500 °C after neutron irradiation was significantly higher than that of Pure W.

As shown in Figs. 14 and 15, irradiation at 910–1010 °C did not induce the hardening of SR W materials, but SR W materials tended to exhibit a decrease in UTS and an increase in TE. It is reported that voids were formed when W was irradiated at 1000 °C, and irradiation at higher temperatures caused the growth of voids and the reduction in the number density of voids [22]. The peak temperature of void swelling in W was 800 °C, and the swelling tended to decrease at higher temperatures [46]. Therefore, irradiation hardening is considered large at temperatures up to 800 °C and is small at 1000 °C in this irradiation campaign. In addition, when exposed to a high-temperature environment of 1000 °C for a long time, it is known that the recrystallization of Pure W (SR) proceeded and induced softening [33]. Comparing the necking deformation of Pure W (SR) before and after irradiation in Fig. 3, while unirradiated Pure W (SR) had primarily deformation in the thickness direction, irradiated Pure W (SR) was characterized by deformations in the thickness and width directions during necking. Pure W (SR) after irradiation at 1000 °C would be recrystallized to have equiaxial grain structures. It is, therefore, considered that the softening due to recovery and recrystallization of SR W materials and

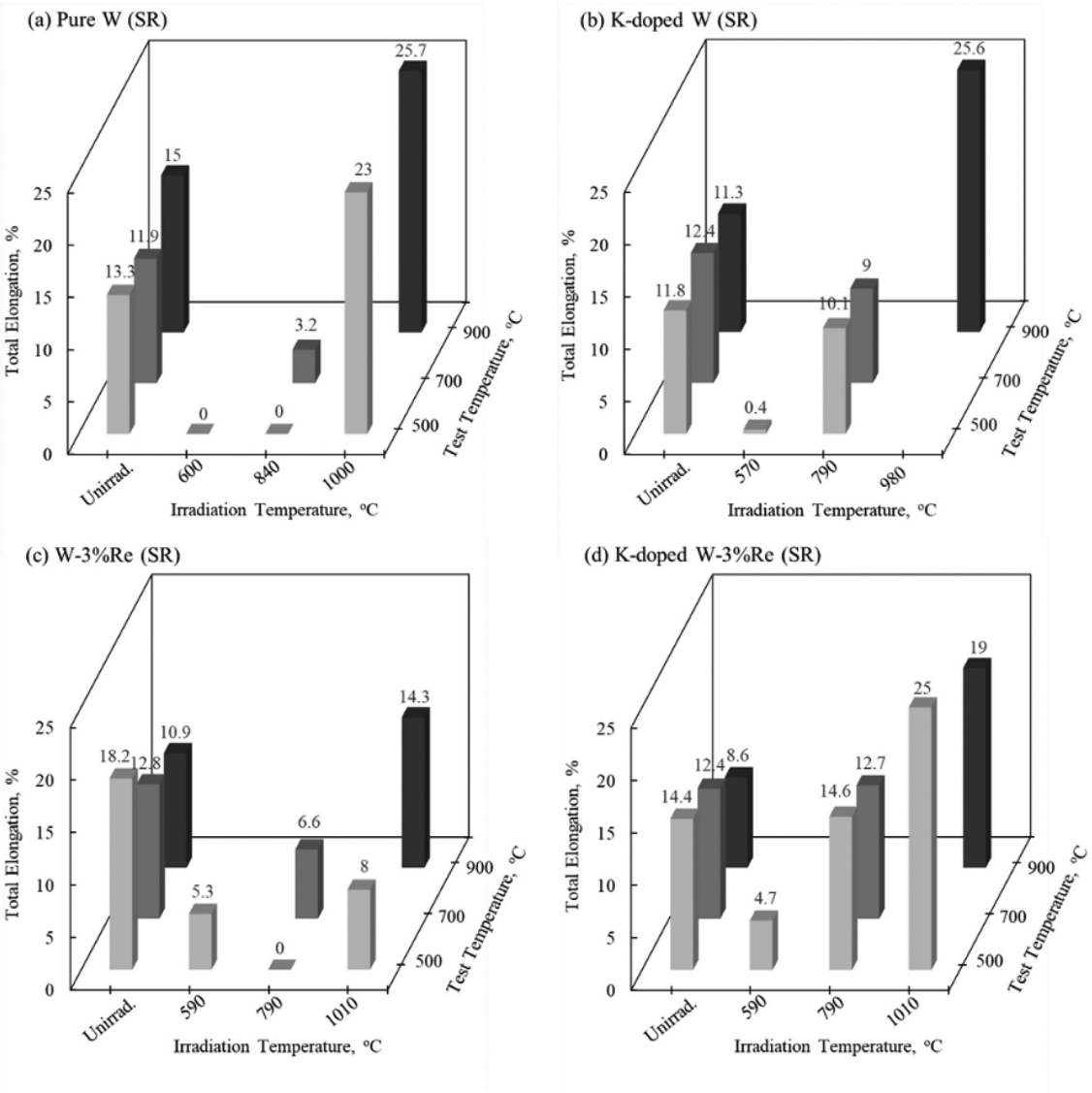

Fig. 15. Dependence of uniform elongation on irradiation temperatures. Test temperatures were about 100 °C lower than the irradiation temperatures. Tensile data of Pure W and its alloys irradiated at ~600 °C and ~800 °C have been published [20].

hardening due to the formation of irradiation defect clusters were balanced during irradiation at 1000 °C, and ductility was exhibited without an increase in strength.

5. Conclusions

High-temperature tensile properties of stress-relieved (SR), thermal aged (TA), and recrystallized (R) Pure W, and its alloys with Re and K were examined after neutron irradiation up to 0.7 dpa at 1000 °C with a thermal neutron shield in an HFIR. The results of this study can be concluded as follows:

After irradiation, Pure W (R) exhibited a brittle fracture mode, while K-doped W-3%Re (R) exhibited a ductile fracture mode when tensile tested at 500 °C. As K-doped W-3%Re (R) has fine grains, it contains a considerable number of grain boundaries that act as sinks for defects formed by neutron irradiation. Solid solute Re in the W matrix could improve not only the mechanical properties of W, but also its resistance to neutron irradiation. A 3%Re addition could improve the ductility of W at 500°C. The ductility of K-doped W-3%Re at 500 °C after neutron irradiation was significantly higher than that of Pure W.

Irradiation at 1000 °C did not induce hardening in SR W materials, but SR W materials tended to exhibit a decrease in UTS and an increase in TE. Softening due to the recovery and recrystallization of SR W materials and hardening due to the formation of irradiation defect clusters were balanced during irradiation at 1000 °C, and ductility was exhibited without an increase in strength.

Declaration of Competing Interest

None.

Acknowledgment

The authors thank the ORNL LAMDA Technical Team for technical assistance. This study was performed as a part of the US–Japan PHENIX Collaboration Project on Technological Assessment of Plasma Facing Components for DEMO Reactors. The ORNL research was sponsored by the U.S. Department of Energy, Office of Fusion Energy Sciences, under contract DE-AC05-00OR22725 with UT-Battelle, LLC. This study was supported by JSPS KAKENHI, Grant Number 17H01364.

References

[1] S. Wurster, N. Baluc, M. Battabyal, T. Crosby, J. Du, C. García-Rosales, A. Hasegawa, A. Hoffmann, A. Kimura, H. Kurishita, R.J. Kurtz, H. Li, S. Noh, J. Reiser, J. Riesch, M. Rieth, W. Setyawan, M. Walter, J.-H. You, R. Pippan, J. Nucl. Mater. 442 (2013) S181–S189.
[2] T. Hirai, F. Escourbiac, S. Carpentier-Chouchana, A. Fedosov, L. Ferrand, T. Jokinen, V. Komarov, A. Kukushkin, M. Merola, R. Mitteau, R.A. Pitts, W. Shu, M. Sugihara, B. Riccardi, S. Suzuki, R. Villari, Fusion Eng. Des. 88 (2013) 1798–1801.
[3] H. Bolt, V. Barabash, G. Federici, J. Linke, A. Loarte, J. Roth, K. Sato, J. Nucl. Mater. 307-311 (2002) 43–52.
[4] A.R. Raffray, R. Nygren, D.G. Whyte, S. Adbel-Khalik, R. Doerner, F. Escourbiac, T. Evans, R.J. Goldston, D.T. Hoelzer, S. Konishi, P. Lorenzetto, M. Merola, R. Neu, P. Norajitra, R.A. Pitts, M. Roedig, T. Rognlien, S. Suzuki, M.S. Tillack, C. Wong, Fusion Eng. Des. 85 (2010) 93–108.
[5] M.S. Tillack, A.R. Raffraya, X.R. Wang, S. Malang, S. Abdel-Khalik, M. Yoda, D. Youchison, Fusion Eng. Des. 86 (2011) 71–98.
[6] K. Tobita, et al., Nucl. Fusion 49 (2009) 075029.
[7] G. Pintsuk, I. Bobin-Vastra, S. Constans, P. Gavila, M. Rödig, B. Riccardi, Fusion Eng. Des. 88 (2013) 1858–1861.
[8] Y. Seki, K. Ezato, S. Suzuki, K. Yokoyama, H. Yamada, T. Hirayama, Fusion Eng. Des. 109–111 (2016) 1148–1152.
[9] S. Nogami, M. Toyota, W. Guan, A. Hasegawa, Y. Ueda, Fusion Eng. Des. 120 (2017) 49–60.
[10] A.V. Babak, Strength Mater. 14 (1982) 1389–1391.
[11] A.V. Babak, E.I. Uskov, Strength Mater. 15 (1983) 667–672.
[12] A.V. Babak, Sov. Powder Metall. Metal Ceram. 22 (1983) 316–318.
[13] Y. Katoh, L.L. Snead, L.M. Garrison, X. Hu, T. Koyanagi, C.M. Parish, P.D. Edmondson, M. Fukuda, T. Hwang, T. Tanaka, A. Hasegawa, J. Nucl. Mater. 520 (2019) 193–207.
[14] J.M. Steichen, J. Nucl. Mater. 60 (1976) 13–19.
[15] I.V. Gorynin, V.A. Ignatov, V.V. Rybin, S.A. Fabritsiev, V.A. Kazakov, V.P. Chakin, V.A. Tsykanov, V.R. Barabash, Y.G. Prokofyev, J. Nucl. Mater. 191–194 (1992) 421–425.
[16] R.C. Rau, J. Moteff, R.L. Ladd, J. Nucl. Mater. 24 (1967) 164–173.
[17] L.M. Garrison, Y. Katoh, J.W. Geringer, M. Akiyoshi, X. Chen, M. Fukuda, A. Hasegawa, T. Hinoki, X. Hu, T. Koyanagi, E. Lang, M. McAlister, J. McDuffee, T. Miyazawa, C. Parish, E. Proehl, N. Reid, J. Robertson, H. Wang, Fusion Sci. Technol. 75 (2019) 499–509.
[18] U.M. Ciucani, W. Pantleon, Fusion Eng. Des. 146 (2019) 814–817.
[19] A. Alfonso, D.J. Jensen, G.N. Luo, W. Pantleon, Fusion Eng. Des. 98-99 (2015) 1924–1928.
[20] T. Miyazawa, L.M. Garrision, J.W. Geringer, M. Fukuda, Y. Katoh, T. Hinoki, A. Hasegawa, J. Nucl. Mater. 529 (2020) 151910.
[21] R.G. Abernethy, J.S.K.-L. Gibson, A. Giannattasio, J.D. Murphy, O. Wouters, S. Bradnam, L.W. Packer, M.R. Gilbert, M. Klimenkov, M. Rieth, H-C. Schneider, C.D. Hardie, S.G. Roberts, D.E.J. Armstrong, J. Nucl. Mater. 527 (2019) 151799.
[22] R.C. Lau, R.L. Ladd, J. Moteff, J. Nucl. Mater. 33 (1969) 324–327.
[23] M. Fukuda, K. Yabuuchi, S. Nogami, A. Hasegawa, T. Tanaka, J. Nucl. Mater. 455 (2014) 460–463.
[24] M. Fukuda, N.A. Kiran Kumar, T. Koyanagi, L.M. Garrison, L.L Snead, Y. Katoh, A. Hasegawa, J. Nucl. Mater. 479 (2016) 249–254.
[25] T. Koyanagi, N.A. Kiran Kumar, T. Hwang, L.M. Garrison, X. Hu, L.L. Snead, Y. Katoh, J. Nucl. Mater. 490 (2017) 66–74.
[26] L.M. Garrison, Y. Katoh, N.A. Kiran Kumar, J. Nucl. Mater. 518 (2019) 208–225.
[27] X. Hu, C.M. Parish, K. Wang, T. Koyanagi, B.P. Eftink, Y. Katoh, Acta Mater. 165 (2019) 51–61.
[28] T. Tanno, A. Hasegawa, J.C. He, M. Fujiwara, S. Nogami, M. Satou, T. Shishido, K. Abe, Mater. Trans. 48 (2007) 2399–2402.
[29] S. Nogami, A. Hasegawa, M. Fukuda, S. Watanabe, J. Reiser, M. Rieth, Fusion Eng. Des. 152 (2020) 111445.
[30] M. Fukuda, S. Nogami, A. Hasegawa, H. Usami, K. Yabuuchi, T. Muroga, Fusion Eng. Des. 89 (2014) 1033–1036.
[31] K. Sasaki, K. Yabuuchi, S. Nogami, A. Hasegawa, J. Nucl. Mater. 461 (2015) 357–364.
[32] K. Sasaki, S. Nogami, M. Fukuda, Y. Katakai, A. Hasegawa, Fusion Eng. Des. 88 (2013) 1735–1738.
[33] K. Tsuchida, T. Miyazawa, A. Hasegawa, S. Nogami, M. Fukuda, Nucl. Mater. Energy 15 (2018) 158–163.
[34] M. Fukuda, S. Nogami, K. Yabuuchi, A. Hasegawa, T. Muroga, Fusion Sci. Technol. 68 (2015) 690–693.
[35] M. Fukuda, T. Tabata, A. Hasegawa, S. Nogami, T. Muroga, Fusion Eng. Des. 109-111 (2016) 1674–1677.
[36] M. Fukuda, A. Hasegawa, S. Nogami, Fusion Eng. Des. 132 (2018) 1–6.
[37] S. Watanabe, S. Nogami, J. Reiser, M. Rieth, S. Sickinger, S. Baumgartner, T. Miyazawa, S. Hasegawa, Fusion Eng. Des. 148 (2019) 111323.
[38] ASTM E112–85, Standard methods for determining the average grain size, in: Annual Book of ASTM Standards Sect. Met. Test Methods and Anal. Proc., 1986, pp. 227–290.
[39] J.L. McDuffee, C.R. Daily, N.O. Cetiner, C.M. Petrie, J.W Geringer, HFIR-MFE-RB-19J thermal and neutronic design, Fusion Reactor Mater. 205 (2016) DOE/ER-0313/60.
[40] J.W. Geringer, J.L. McDuffee, C.M. Petrie, L.M. Garrison, R.H. Howard, N.O. Cetiner, D.A. Stringfield, R.G. Sitterson, HFIR-MFE-RB-19J specimen loading listing, Fusion Reactor Mater. 215 (2016) DOE/ER-0313/60.
[41] M.E. Sawan, Fusion Eng. Des. 87 (2012) 551–555.
[42] Y. Katoh, in: Proceedings of the 19th International Conference Fusion Reactor Materials (ICFRM-19), La Jolla, California, 2019.
[43] D.B. Snow, Metall. Trans. A 10 (1979) 815–821.
[44] P.L. Raffo, J. Less-Common Met. 17 (1969) 133–149.
[45] A. Hasegawa, M. Fukuda, K. Yabuuchi, S. Nogami, J. Nucl. Mater. 471 (2016) 175–183.
[46] J. Matolich, H. Hahm, J. Moteff, Scr. Metall. 8 (1974) 837–842.